(115)

Photovoltaic spatial solitons

Mordechai Segev

Department of Electrical Engineering and Center for Photonics and Optoelectronic Materials and the Princeton Materials Institute, Princeton University, Princeton, New Jersey 08544

George C. Valley

Hughes Research Laboratories, Malibu, California 90265

Matthew C. Bashaw

Department of Electrical Engineering, Stanford University, Stanford, California 94305, and Silicon Valley Photonics, Menlo Park, California 94025

Minoru Taya* and Martin M. Fejer

E. L. Ginzton Laboratory, Stanford University, Stanford, California 94305

Received November 15, 1996; revised manuscript received January 31, 1997

We analyze self-trapping of one-dimensional optical beams in photorefractive, photovoltaic media for open- and closed-circuit realizations. We show that a passive load (resistor) in the external circuit can be used for switching of dark photovoltaic solitons. Dark solitons in a short-circuited crystal can be obtained for a much smaller nonlinearity than in open-circuit conditions. Shorting the crystal affects bright solitons very little.
 [S0740-3224(97)00207-5]

1. INTRODUCTION

Photorefractive spatial solitons[1] have attracted much interest in the past few years.[2–36] It is now well established that photorefractive nonlinearities can support self-trapping of optical beams in both transverse dimensions and that these solitons can be observed even at very low power levels (microwatts and lower). At present, several generic types of photorefractive soliton are known: quasi-steady-state solitons,[2–11] screening solitons,[12,33] and photovoltaic solitons,[34–36] all of which can form in dielectric photorefractive crystals, and resonant self-trapping, which is unique to photorefractive semiconductors.[37] Following the initial observations of each type of soliton, recent attention has been paid to vector solitons and soliton pairs[27–33] and to soliton collisions.[24–26] Finally, a recent observation has been reported of self-trapping of a partially spatially incoherent beam,[38] which was explained theoretically by a quasi-particles approach.[39]

In this paper we revisit one-dimensional bright and dark photovoltaic solitons and analyze their formation under open- and closed-circuit realizations. We show that the open-circuit photovoltaic solitons resemble solitons in saturable Kerr nonlinearities.[40] This similarity is removed when current is allowed to flow in the external circuit. We determine the current as a function of the illumination (amplitude and structure), crystal parameters, and the external resistance. Finally, we find bright and dark solitons in the closed-circuit configuration and discuss the possibility of switching by use of the external resistor.

2. GENERAL TREATMENT

We start with the standard set of rate and continuity equations and Gauss's law, which describe the photorefractive effect in a medium in which the photovoltaic current is nonzero and electrons are the sole charge carriers, plus the scalar wave equation for the slowly varying amplitude of the optical field. In steady state and two dimensions these equations are[34,41]

$$(s|A|^2 + \beta)(N_d - N_d^{\,i}) - \gamma \hat{n} N_d^{\,i} = 0, \tag{1}$$

$$\nabla \cdot \hat{\mathbf{J}} = \nabla \cdot [q\mu \hat{n}\hat{\mathbf{E}} + k_B T \mu \nabla \hat{n} + \kappa_{\text{eff}}(N_d - N_d^{\,i})|A|^2 \hat{\mathbf{z}}] = 0, \tag{2}$$

$$\nabla \cdot \hat{\mathbf{E}} + (q/\varepsilon_s)(\hat{n} + N_A - N_d^{\,i}) = 0, \tag{3}$$

$$\left(\frac{\partial}{\partial z} - \frac{i}{2k}\frac{\partial^2}{\partial x^2}\right) A(x, z) = \frac{ik}{n_b}\Delta n(\hat{\mathbf{E}}) A(x, z), \tag{4}$$

where $\Delta n(\hat{\mathbf{E}}) = -0.5 n_b^{\,3} r_{\text{eff}} \hat{\mathbf{E}}$ is the perturbation in the refractive index and the independent variables are z, the propagation axis, and x, the transverse coordinate. The five dependent variables are $\hat{n}$, the electron number density; $N_d^{\,i}$, the number density of ionized donors; $\hat{\mathbf{J}}$, the current density; $\hat{\mathbf{E}}$, the space-charge field inside the crystal; and A, the slowly varying amplitude of the optical field, defined by $E_{\text{opt}}(x, z, t) = A(x, z)\exp(ikz - i\omega t)$ + c.c. ($k = 2\pi n_b/\lambda$, and ω is the frequency). Relevant parameters of the crystal are N_d, the total donor number density; N_A, the number density of negatively charged acceptors that compensate for the ionized donors; β, the dark generation rate; s, the photoionization cross section;

0740-3224/97/0701772-10$10.00

γ, the recombination coefficient; μ, the electron mobility; ϵ_s, the low-frequency dielectric constant; r_{eff}, the effective electro-optic coefficient; and κ_{eff}, the effective photovoltaic constant. $-q$ is the charge on the electron, k_B is Boltzmann's constant, and T is the absolute temperature. Note that κ_{eff} is in units of (A cm sc) and is related to the photovoltaic constant κ of Ref. 42 through $\kappa_{\text{eff}} = \kappa(h\nu)$, where $h\nu$ is the energy of an individual photon contributing to the photovoltaic current and to the photovoltaic constant β of Ref. 43 through $\beta = s\kappa_{\text{eff}}$. Finally, we define the optical and the dark irradiances as $I = |A|^2$ and $I_{\text{dark}} = \beta/s$, respectively.

We point out that, in principle, one could add uniform illumination to increase the uniform background number density of electrons, in a manner similar to screening solitons. The reason for this as follows: The available nonlinear response is maximized, for bright screening solitons[15] and for both bright and dark open-circuit photovoltaic solitons,[34] when the maximum intensity of the soliton is comparable with I_{dark}. However, I_{dark} is typically very small (mW/cm^2) in all oxide and sillenite photovoltaic–photorefractive materials. This results in very long response time (minutes or more) because the dielectric relaxation time is inversely proportional to the sum of the optical and the dark irradiances. Additional uniform illumination (so-called background irradiance) can be equivalent to effectively increasing I_{dark}, thus providing additional control over the photorefractive nonlinearity and permitting observation of microwatt solitons with 0.1-s response times in strontium barium niobate (see Ref. 15 for the theoretical background; all the experiments described in Refs. 16–26, 32, and 33 have used this idea in conjunction with screening solitons). It is most convenient, however, to use this additional (uniform) background illumination when the background beam itself is not affected by the material nonlinearity and when the background beam does not induce additional nonlinear effects beyond simply increasing the background carrier density. For screening solitons these conditions can easily be obtained in most photorefractive crystals with a beam that is orthogonally polarized to the soliton beam,[15] although some small nonlinear effects are apparent on the background beam.[19] In photovoltaic media the issue is more complicated because the background beam can induce an additional photovoltaic current [an additional constant term in Eq. (2)]. In fact, this is the situation with photovoltaic $LiNbO_3$, for which the photovoltaic coefficients for extraordinarily and ordinarily polarized light are comparable.[44]

Equations (1)–(4) are supplemented by the relation between the space-charge field $\hat{\mathbf{E}}$ and the current flowing in the circuit:

$$V = -\int_{-l/2}^{l/2} \hat{\mathbf{E}} \cdot \mathrm{d}l = RS\hat{\mathbf{J}}, \tag{5}$$

where V is the potential measured between the crystal's electrodes separated by l, S is the surface area of the electrodes, and R is the external resistance.

We look for stationary (nondiffracting) solutions of the form

$$A(x, z) = u(x)\exp(i\Gamma z)\sqrt{I_{\text{dark}}}, \tag{6}$$

where Γ is the soliton propagation constant. We limit our analysis to real $u(x)$.[45] Inasmuch as $I = |A|^2$ depends on x alone, we look for solutions in which the dependent variables, n, $N_d{}^i$, $\hat{\mathbf{J}}$, and $\hat{\mathbf{E}}$ depend solely on x and the only component of $\hat{\mathbf{E}}$ and $\hat{\mathbf{J}}$ is in the x direction. The simplest case is that in which the polarization of the optical beam and the propagation directions with respect to the crystalline axes are chosen such that the effective electro-optic and photovoltaic coefficients are $r_{\text{eff}} = r_{iii}$ and $\kappa_{\text{eff}} = \kappa_{iii}$, where i is a principal axis parallel to x.[46] This configuration is illustrated in Fig. 1.

Next, we define the dimensionless parameter $a \equiv sI_{\text{dark}}/(\gamma N_A)$, which scales the optical (+thermal) excitation with respect to the recombination rate, where $\tau_R = 1/(\gamma N_A)$ is the recombination time. We now transform the equations into dimensionless form by the substitutions $n = \hat{n}/(aN_d)$, $r = N_d/N_A$, $N = N_d{}^i/N_d$, $E = \hat{\mathbf{E}}/E_p$, and $J = \hat{\mathbf{J}}/(q\mu aN_dE_p)$, where $E_p = \kappa_{\text{eff}}\gamma N_A/(q\mu) = \kappa_{\text{eff}}/(q\mu\tau_R)$, $\xi = x/d$, $d = (\pm 2kb)^{-1/2}$ is the characteristic length scale, and $b = (k/n_b) \times (0.5n_b{}^3r_{\text{eff}}E_p)$ is the parameter that characterizes the strength and the sign of the optical nonlinearity. In this notation the unknowns that characterize the material's response, n, N, E, and J, are all of order unity. Notice that $d = \lambda/[2\pi(\pm 2\Delta n_0 n_b)^{1/2}]$, where $\Delta n_0 = 0.5n_b{}^3r_{\text{eff}}E_p$ is the electro-optic change in the refractive index induced by an external (bias) electric field of amplitude E_p and λ is the vacuum wavelength. The sign of r_{eff} and κ_{eff} determines the sign (positive or negative) of Δn_0. We therefore introduce the dual-sign ($\pm$) notation in the definition of d, where the upper and the lower signs apply to positive and negative values, respectively, of b (and, consequently, of Δn_0). Note that the photovoltaic term in the current [the last term on the right-hand side of Eq. (2)] is proportional to $|A|^2$ and not to I_{dark}. This is true for a fundamental reason: The photovoltaic current is proportional to real illumination and not to thermal excitations; i.e., there is no thermal photovoltaic current.[47]

The dimensionless equations are

$$n - (1 + u^2)(1 - N)/(rN) = 0, \tag{7}$$

$$J = nE + (1 - N)u^2 + \epsilon_1(\mathrm{d}n/\mathrm{d}\xi) = \text{const.}, \tag{8}$$

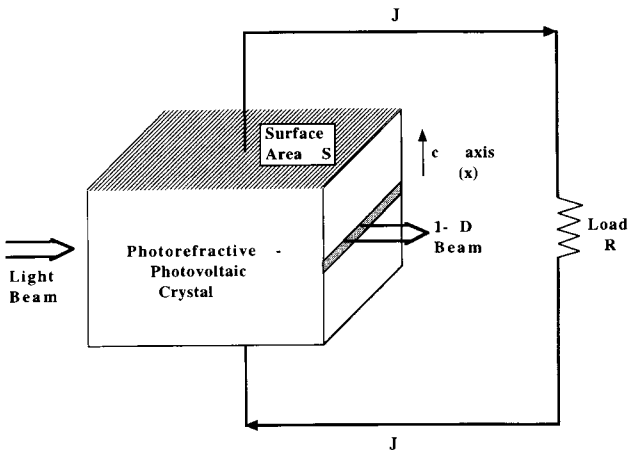

Fig. 1. Illustration of the electrical circuit consisting of a photovoltaic crystal (acting as a source when illuminated) and an external resistor R. 1-D, one-dimensional.

$$(N - 1/r - an) - \varepsilon_2(\mathrm{d}E/\mathrm{d}\xi) = 0, \tag{9}$$

$$\mathrm{d}^2u/\mathrm{d}\xi^2 = \pm(\Gamma/b + E)u, \tag{10}$$

$$J = -\beta \int_{-l/2d}^{l/2d} E(\xi)\mathrm{d}\xi, \tag{11}$$

where $\varepsilon_1 = \mu k_B T \tau_R/(\kappa_{\mathrm{eff}} d)$ and $\varepsilon_2 = \varepsilon_s \kappa_{\mathrm{eff}}/(q^2 \mu d \tau_R N_d)$ are both dimensionless parameters and $\beta = d/(RSq\mu a N_d)$. It is now important to obtain some quantitative values of the parameters involved. We therefore consider typical parameters of $LiNbO_3$ in a configuration that can give rise to an index change $\Delta n_0 \approx 5 \times 10^{-4}$ that is sufficiently large to support an ~10-μm-wide soliton at $\lambda \approx 0.5$ μm.[15,35] Recalling that $n_b = n_e \approx 2.27$ and $r_{33} \approx 32 \times 10^{-12}$ m/V, we find that the value of E_p required for support of such Δn_0 is $E_p \approx 27$ kV/cm, which is easily attainable in $LiNbO_3$ (in fact, photovoltaic space-charge fields up to 250 kV/cm and Δn_0 up to 0.003 have been measured[48] in $LiNbO_3$). When the values in Refs. 42 and 43 are used, similar values correspond to $LiNbO_3$:0.2% Fe, with electron mobility $\mu \approx 0.01$ [$\mathrm{cm^2\ V^{-1}\ s^{-1}}$], $\tau_R \approx 27.6$ ps, and $\kappa_{\mathrm{eff}} \approx 12 \times 10^{-28}$ [A cm s] (or $\kappa \approx 3 \times 10^{-9}$ in the [A cm/W] units of Ref. 42). This implies that for typical values[44] of $I_{\mathrm{dark}} \approx 1$ mW/cm^2 and $s \approx 3.6$[$\mathrm{cm^2\ s^{-1}\ W^{-1}}$], we get $a = 10^{-13}$. Further, for $E_p = 27$ kV/cm we get $d \approx 1.67$ μm. At room temperature, $T = 300$ K, we find that $\varepsilon_1 = 0.005$, and with typical $LiNbO_3$ values of $\varepsilon_s \approx 30\varepsilon_0$ and $N_d \approx 10^{18}$ cm^{-3} we obtain $\varepsilon_2 = 0.0027$.

With these parameters in mind we revisit Eqs. (7)–(11). First, we recall that $N \leqslant 1/r \ll 1$ for light intensities much smaller than 1 MW/cm^2. Using this inequality in Eq. (7) provides $n \cong (1 + u^2)/(rN)$. Examining the terms in Eq. (8) reveals that, because E is of the order of unity, the last term in Eq. (8) is much smaller than the first two and can be neglected whenever $(\mathrm{d}n/\mathrm{d}\xi) \ll 200$ [because $nE \sim (1 + u^2)$ and $(1 - N)u^2 \sim u^2$, whereas $\varepsilon_1(\mathrm{d}n/\mathrm{d}\xi) \sim 0.005(1 + u^2)$]. Furthermore, in Eq. (9) we can neglect both terms $(an) \approx 10^{13}(1 + u^2)$ and $\varepsilon_2(\mathrm{d}E/\mathrm{d}\xi)$ and obtain $N \approx 1/r = N_A/N_d \approx 0.05$ [whenever $(\mathrm{d}E/\mathrm{d}\xi) \ll 20$]. This means that, to the lowest order of our approximation, $N \approx 1/r = N_A/N_d \approx 0.05$; i.e., the number density of ionized donors equals the density of acceptors N_A, which is a constant and does not vary with x. Corrections to these approximations (to any desired order in the smallness parameters ε_1 and ε_2) can be obtained by use of an asymptotic expansion similar to that of Ref. 15. For our choice of parameters the approximations can easily be justified *a posteriori*, that is, after we solve for solitons and find the actual waveforms.[49] These approximations can be used in Eq. (8) and yield

$$J = nE + (1 - 1/r)u^2 \approx nE + u^2 = (1 + u^2)E + u^2 = \text{const.} \tag{12}$$

Finally, we obtain for the space-charge field $E(\xi)$

$$E(\xi) = \frac{J - u^2(\xi)}{[1 + u^2(\xi)]}, \tag{13}$$

which, when substituted into Eq. (10), gives the nonlinear wave equation that describes stationary (soliton) propagation in this photovoltaic nonlinear medium:

$$\frac{\mathrm{d}^2u}{\mathrm{d}\xi^2} = \pm\left(\frac{\Gamma}{b} + \frac{J - u^2}{(1 + u^2)}\right)u. \tag{14}$$

The solutions of Eq. (14), $u(\xi)$ with the appropriate boundary conditions, are bright and dark solitons.

So far the current J has been unspecified. Although J is a constant, it is determined not only by constant quantities, such as the parameters of the external circuit (R and S) and of the crystal (a, μ, d, and N_d), all incorporated into one constant β, but also by the waveform of the optical beam. In principle, one should solve Eqs. (14) and (11) in a self-consistent manner. A traditional approach to solving such problems is to use numerical relaxation methods (which are commonly used to solve a related self-consistency problem of Schrödinger's and Poisson's equations together). In Section 3 we provide a simple method to evaluate the constant current J without resorting to an extensive numeric calculation.

3. EVALUATION OF THE CURRENT

Here we evaluate the optically induced current that flows through the photovoltaic crystal and the external (passive) resistor connected in series. At steady state, the continuity equation [Eq. (2)] implies that the current is constant everywhere, including regions in which the optical intensity distribution varies with the coordinates. By substituting the expression for $E(\xi)$ [Eq. (13)] into the relation defined by Eq. (11), we find that

$$J = -\beta \int_{-l/2d}^{l/2d} \frac{J - u^2(\xi)}{[1 + u^2(\xi)]}\,\mathrm{d}\xi. \tag{15}$$

We now examine three different cases of optical intensity distribution: uniform illumination, dark solitons, and bright solitons.

A. Uniform Illumination

Consider first a uniform beam, polarized at the proper polarization, that gives rise to nonvanishing photovoltaic current (through a nonzero κ_{eff}) of normalized intensity $u^2(\xi) = u_\infty^2$ for all ξ. The integral in Eq. (15) leads to

$$J = \frac{\left(\frac{\beta l}{d}\right)u_\infty^2}{1 + u_\infty^2 + \left(\frac{\beta l}{d}\right)}. \tag{16}$$

We note two limiting cases. The first occurs when the external resistor is infinite (open-circuit conditions), i.e., $R \to \infty$. In this case $\beta \to 0$, which implies that $J = 0$ and the current is simply zero. The second limiting case occurs when the electrodes are connected by a perfect conductor, i.e., $R \to 0$. Then $(\beta l/d) \gg 1 + u_\infty^2$, and we get $J = u_\infty^2$. This means that, although the resistance in the external circuit is zero, the available current is limited by the photovoltaic crystal (which acts as a current source) illuminated at a specific intensity.

Using the above parameters of $LiNbO_3$ at $u_\infty^2 = 1000$ and $I_{dark} = 1\ mW/cm^2$, we find the maximum short-circuit current, $\hat{J}_{max} \approx 4\ nA/cm^2$. For the current to be at this limit it is sufficient to require that the external resistance be much smaller than $10^{13}\Omega$ (assuming even much smaller resistance of the electrodes), which is easily attainable.

B. Dark Solitons

Consider now a dark solitonlike beam of width Δx and peak intensity u_∞^2, as illustrated in Fig. 2(a). Assuming that the dark notch borne on this beam has a square shape, one can perform the integral of Eq. (15) and obtain, in the limit $l \gg \Delta x$,

$$J \cong \frac{\left(\frac{\beta l}{d}\right) u_\infty^2}{(1 + u_\infty^2)\left(1 + \frac{\beta \Delta x}{d}\right) + \left(\frac{\beta l}{d}\right)}. \tag{17}$$

Once again, it is instructive to discuss limiting cases. The first case is again simple: $R \to \infty$, which implies that $\beta \to 0$ and $J = 0$; i.e., no current flows through the crystal (open-circuit configuration). The second limiting case is $R \to 0$, which gives $J \to l u_\infty^2/[(1 + u_\infty^2)\Delta x + l]$. Using typical values for the dimensions of the crystal ($l \approx 5$ mm) and the size of the notch ($\Delta x \approx 5\ \mu m$), we find that whenever $u_\infty^2 \ll 1000$, $J \approx u_\infty^2$, whereas when $u_\infty^2 \gg 1000$, $J \approx l/\Delta x \sim 1000$.

C. Bright Solitons

Consider now a bright solitonlike beam of width Δx and peak intensity u_0^2, as illustrated in Fig. 2(b). Assuming that the beam has a square shape, one can perform the integral of Eq. (15) and obtain, in the limit $l \gg \Delta x$,

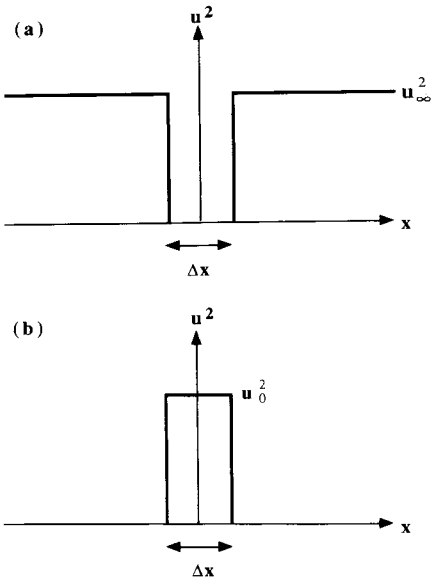

Fig. 2. (a) Dark solitonlike beam of width Δx and peak intensity u_∞^2. (b) Bright solitonlike beam of width Δx and peak intensity u_0^2.

$$J \cong \frac{\left(\frac{\beta \Delta x}{d}\right) u_\infty^2}{(1 + u_0^2)\left(1 + \frac{\beta l}{d}\right) + \frac{\beta \Delta x}{d}}. \tag{18}$$

The limiting cases now give (i) $R \to \infty$, which implies that $\beta \to 0$ and $J = 0$, i.e., no current flows through the crystal (open-circuit configuration), and (ii) $R \to 0$, which gives $J \to (\Delta x u_0^2)/[\Delta x + l(1 + u_0^2)]$. Because $l \gg \Delta x$, $J \to (\Delta x u_0^2)/[l(1 + u_0^2)] \leqslant \Delta x/l \approx 0.001$.

We point out that in all three cases (uniform illumination and dark and bright solitonlike beams), the current is positive. This implies that in all cases the photovoltaic crystal acts as a current source, with current flowing from its positive electrode. This does not mean that the polarity of the field inside the crystal is the same in all three cases. On the contrary: it varies from one case to another. With the above estimates for J, we can now rewrite the explicit space-charge field $E(\xi)$, using Eq. (13) in the three different cases of uniform illumination, dark solitons, and bright solitons. We find that whenever the external resistance is very large ($R \to \infty$), $J \to 0$ and

$$E(\xi) = \frac{-u^2(\xi)}{[1 + u^2(\xi)]} \tag{19}$$

for all three cases (this result coincides with that for the case discussed in Ref. 34). However, when the external resistance is very small ($R \to 0$), the cases differ from one another considerably, even though the current in all three cases is positive ($J \geqslant 0$).

First, consider the case of uniform illumination with intensity u_∞^2 everywhere and $R \to 0$. If we use the approximation $(\beta l/d) \gg 1 + u_\infty^2$ [below Eq. (16)], which leads to $J \cong u_\infty^2$, we get [by substituting the approximation into Eq. (13)] $E(\xi) = 0$ for all ξ. Obviously, this is incorrect because whenever current flows ($J \neq 0$) the field cannot be zero. The correct substitution is to use the full expression for J from Eq. (16) in the expression for $E(\xi)$ of Eq. (13). This leads to $E = -u_\infty^2/(1 + u_\infty^2 + \beta l/d)$, which goes to zero for large β (small R). Note that in both limiting cases of $R \to 0$ and $R \to \infty$ the field everywhere in the crystal is limited by the crystal itself, which acts as a source. The field in both cases is negative.

Second, consider the field $E(\xi)$ for $R \to 0$ in the case of illumination with a dark notch [Fig. 2(a)]. We find that

$$E(\xi) = \frac{l[u_\infty^2 - u^2(\xi)] - \Delta x(1 + u_\infty^2)u^2(\xi)}{[1 + u^2(\xi)][(1 + u_\infty^2)\Delta x + l]}. \tag{20}$$

It is now instructive to look at two different locations in the dark-notch-bearing beam. At $\xi = 0$ [where $u(0) = 0$] we find that $E(0) = J > 0$. However, at $\xi \to \infty$ (where $u^2 = u_\infty^2$) we find that $E(\xi \to \infty) = -u_\infty^2 \Delta x/[(1 + u_\infty^2)\Delta x + l] < 0$. This implies that, at some value of ξ, $E(\xi)$ changes sign. This feature is important when one calculates the profiles of the dark solitons (for the closed-circuit configuration) and derives the refractive-index profiles that support (self-trap) them.

Third, for bright steplike beams [Fig. 2(b)], the field for $R \to 0$ is

$$E(\xi) = \left[\frac{\Delta x u_0^2}{l(1+u_0^2)} - u^2(\xi)\right] \Big/ [1+u^2(\xi)]. \quad (21)$$

At $\xi = 0$ [where $u(0) = u_0$], $E(0)$ is always negative. However, if we look at $\xi \to \infty$ (where $u^2 = 0$), we find that $E(\xi \to \infty) = J = \Delta x/[l(1+u_0^2)] > 0$. Similar to the case of closed-circuit dark solitons, at some coordinate ξ, $E(\xi)$ must change sign.

As a concluding remark to this section, we point out that the simple method that we used to evaluate the current for the cases of dark and bright solitonlike beams provides only a rough estimate. A more accurate estimate of the current in those cases can be made with the method used in the appendixes of Refs. 12 and 15 for screening solitons, which employs the quadrature relation (described in Section 4) in evaluating the integral of Eq. (15), without the need to compute the waveforms of the solitons first. An even more accurate method would be to calculate J in a self-consistent manner, which requires numerical methods. When comparing the various methods we find, however, that the estimation methods are accurate for a fairly large range of intensity ratios and $\Delta x/l \ll 1$ (e.g., comparing the estimates for screening solitons as described in Refs. 12 and 15 with the numerical methods for the same problem that are used in Ref. 13 gives the same result with less than 10^{-4} error for bright solitons and less than 10^{-3} error for dark solitons). With this understanding in hand, we proceed to Section 4 and look for soliton solutions.

4. SOLITONS: GENERAL TREATMENT

We provide the general treatment that is common to both dark and bright solitons. We start with Eq. (14).

$$u'' = \pm\left(\delta + \frac{J-u^2}{1+u^2}\right)u, \quad (22)$$

where the double prime stands for the derivative with respect to the variable ξ, $\delta = \Gamma/b$, and the upper (lower) sign indicates $\Delta n_0 > 0$ (< 0). We integrate Eq. (22), using quadrature, and obtain

$$p^2 - p_0^2 = \pm\left[(\delta-1)(u^2-u_0^2) + (J+1) \times \ln\left(\frac{u^2+1}{u_0^2+1}\right)\right], \quad (23)$$

where $p = u'$, $p_0 = p(\xi = 0)$, and $u_0 = u(0)$.

We point out that one-dimensional beam propagation in open-circuit photovoltaic media (the $J = 0$ case) is mathematically identical to that in saturable nonlinear Kerr media,[40] and thus the features of soliton collisions should be identical.[50] However, when the current is nonzero (closed circuit) the nonlinearity changes, and the similarity no longer holds. This result has a dramatic effect on dark solitons because of the large photoinduced current, whereas bright solitons are hardly affected (because the current for bright solitons is small). Another interesting observation is that, despite the inherent nonlocality in the physics of the photorefractive and photovoltaic effects (as manifested in charge transport: electrons photoexcited at one point move to another point where they are retrapped, and the space-charge field results from the charges' being separated) the steady-state single-beam optical photovoltaic effects are local (at least within the regime of our approximations) for both open- and closed-circuit cases. That is, the photoinduced change in the refractive index $\Delta n(x)$ at a specific coordinate x is a function of the light intensity at that particular coordinate $I(x)$ only.

5. DARK SOLITONS

For dark solitons one requires the boundary conditions (i) $u(\infty) = u_\infty \neq 0$, (ii) $u'(\infty) = u''(\infty) = 0$, (iii) $u_0 = 0$, and (iv) a real (nonzero) p_0. The first two conditions ensure a constant value of the wave function far from $\xi = 0$; the last eliminates solutions that are periodic in ξ. Using boundary conditions (i) and (ii) and substituting $\xi \to \infty$ into Eq. (22) lead to $\delta = (u_\infty^2 - J)/(1+u_\infty^2)$. As explained above, J is always positive, which implies that $0 \leq \delta < 1$, that the propagation constant Γ depends on u_∞, and that its sign is identical to that of Δn_0 for all values of u_∞ and J. This situation is in contrast to that for dark screening solitons,[15] which all have the same propagation constant regardless of their peak intensity u_∞^2. Substituting conditions (i)–(iii), the expression we have just found for δ, and $\xi \to \infty$ into Eq. (23) leads to

$$p_0^2 = \pm\left\{(J+1)\left[\frac{u_\infty^2}{1+u_\infty^2} - \ln(u_\infty^2+1)\right]\right\}. \quad (24)$$

The reality of p_0 [condition (iv)] can be obtained only for the lower sign, implying that dark solitons can be generated by use of a negative Δn_0 only. Nevertheless, a dark photovoltaic soliton induces a waveguide structure in the region of the dark notch in which a second (bright) beam can be guided efficiently and switched on and off.[35,36] Therefore photovoltaic dark solitons are solutions of

$$u'' = -\left(\delta + \frac{J-u^2}{1+u^2}\right)u, \quad (25)$$

with $u(0) = 0$, $u'(0) = p_0 = \{(J+1)[\ln(u_\infty^2+1) - (u_\infty^2)/(u_\infty^2+1)]\}^{1/2}$, and $\delta = (u_\infty^2 - J)/(1+u_\infty^2)$, or, alternatively, of

$$u' = \left\{(J+1)\left[\frac{u^2-u_\infty^2}{1+u_\infty^2} + \ln\left(\frac{1+u_\infty^2}{1+u^2}\right)\right]\right\}^{1/2}, \quad (26)$$

with $u(0) = 0$.

Recall now that J can vary continuously from zero (at $R \to \infty$) to the maximum value of $J = J_{\max} \to lu_\infty^2/[(1+u_\infty^2)\Delta x + l]$ (at $R \to 0$). In what follows we analyze only these limiting cases, keeping in mind that all intermediate cases can be calculated in a similar manner. We integrate Eq. (26) numerically for various values of u_∞, $J = 0$, and $J = J_{\max}$ and obtain the waveforms $u(\xi)$ of

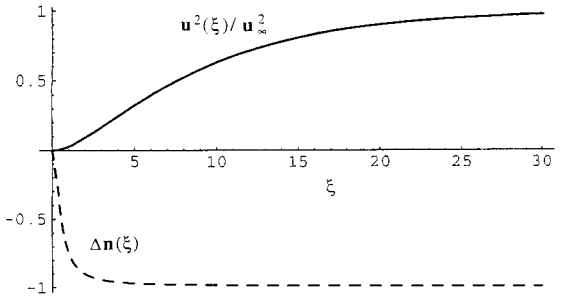

Fig. 3. Normalized intensity profile (solid curve) of the open-circuit dark photovoltaic soliton and the induced change in the refractive index [$\Delta n(\xi) \propto E(\xi)$; dashed curve], both at $u_\infty = 10$ and $J = 0$.

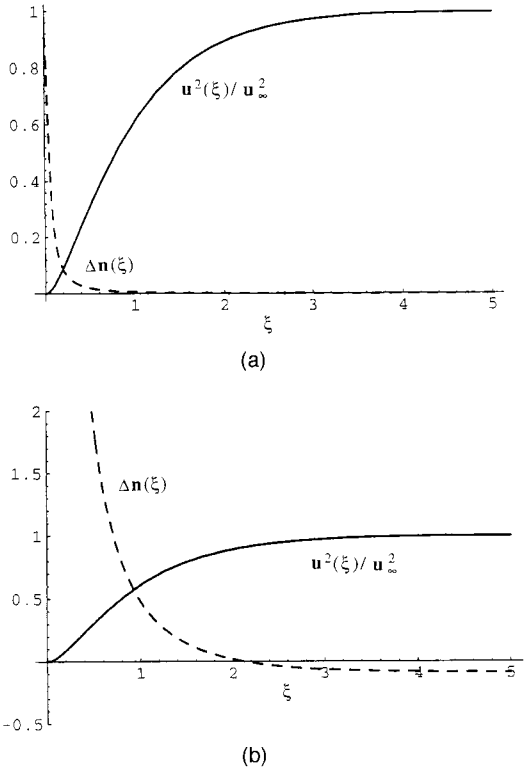

Fig. 4. (a) Normalized intensity profile (solid curve) of the closed-circuit dark photovoltaic soliton and the induced change in the refractive index [$\Delta n(\xi) \propto E(\xi)$, dashed curve], both at $u_\infty = 10$ and $J = J_{max}$. (b) Expanded version of (a).

dark photovoltaic solitons. Particular cases of $u_\infty = 10$ with $J = 0$ and $J = J_{max}$ are shown in Figs. 3 and 4, respectively. We have assumed that $\Delta x/l = 0.001$ (corresponding to a 5-μm-wide soliton in a 5-mm-wide crystal). Figure 3 shows the intensity waveform (solid curve) of the open-circuit dark photovoltaic soliton and the induced change in the refractive index [$\Delta n(\xi) \propto -|E(\xi)|$; dashed curve] between $\xi = 0$ and $\xi = 30$. Notice that $\Delta n(\xi)$ is negative for all ξ. Nevertheless, it forms an effective graded-index waveguide that can guide another beam, as observed in Refs. 35 and 36. The situation becomes very different for $J = J_{max}$ and the same intensity ratio $u_\infty = 10$. Figure 4(a) shows the intensity waveform (solid curve) of the closed-circuit dark photovoltaic soliton and the induced change in the refractive index (dashed curve) between $\xi = 0$ and $\xi = 5$. Figure 4(b) is an expanded version of the same figure.

Several new features of photovoltaic solitons with an external circuit are now apparent. First, the dark soliton is much narrower in the closed-circuit case than in the open-circuit case. This means that a lower nonlinearity (Δn_0) is now sufficient to self-trap a soliton of the same width in the same medium (which, of course, has the same λ, n_b, κ_{eff}, and r_{eff}). Furthermore, whereas the asymptotic value of $\Delta n(\xi)$ at $\xi \to \infty$ (or near the electrodes) is negative in both cases, in the J_{max} case Δn changes sign at the vicinity of $\xi = 0$ and becomes very large there. This means that the space-charge field $E(\xi)$ changes sign and becomes positive near the center of the dark notch. The narrow and steep shape of Δn in this case gives rise to a much narrower dark soliton (and to a much narrower induced waveguide) in the J_{max} case than in the $J = 0$ case.

The large difference between the behavior of dark solitons at zero and maximum current strongly depends on the peak soliton intensity ratio, u_∞^2. For example, at a low intensity ratio, such as that of $u_\infty^2 = 0.01$, the waveforms of the dark solitons $u(\xi)$ and their induced $\Delta n(\xi)$ for $J = J_{max}$ coincide with those for $J = 0$ (see Fig. 5). The functional behavior of the width of the dark soliton as a function of the soliton's peak amplitude u_∞ can be calculated by use of numerical integration of Eq. (26). The result is shown in Fig. 6, where we plot the soliton's full width at half-maximum of u^2 as a function of the ratio between its peak amplitude and the square root of the background irradiance (u_∞). The curves show $J = 0$ and $J = J_{max}$. Notice that for small values of u_∞ the two curves coincide, as can be observed for the particular case of $u_\infty = 0.1$ of Fig. 5. On the other hand, the fast increase of the normalized soliton width as a function of u_∞, which is characteristic of saturable Kerr nonlinearities[40] and is present in the $J = 0$ case, is restrained by the existence of current through the crystal. The current gives rise to much slower saturation, which is manifested in a much slower growth of the soliton width as a function of u_∞ (although it never reaches the full arrest of saturation that is present in dark screening solitons, as manifested in their asymptotically constant existence curve at $u_\infty \gg 1$).

We point out that the functions shown in Fig. 6 provide the soliton existence curves and emphasize that for a one-

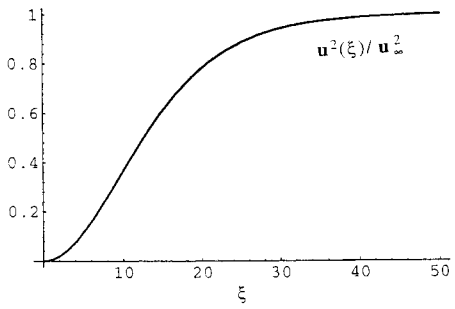

Fig. 5. Normalized intensity profile of dark solitons at $u_\infty = 0.1$ for both $J = 0$ and $J = J_{max}$. The profiles coincide everywhere.

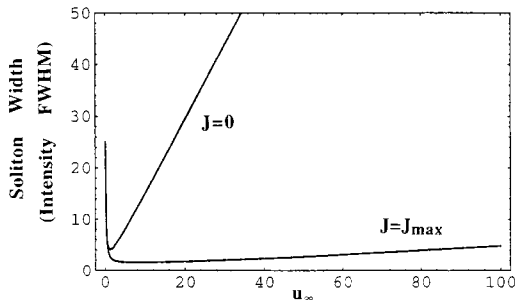

Fig. 6. Soliton existence curve for open-circuit (upper curve) and closed-circuit (lower curve) dark photovoltaic solitons. The curves show the soliton width (FWHM of the intensity, u^2) in units of $\Delta x k_0 n_b^2 (r_{\text{eff}} E_p r)^{1/2}$ as a function of the peak soliton amplitude u_∞, k_0 being the wave number in vacuum.

dimensional photovoltaic soliton at any particular (allowed) value of current there exists a unique relation between the soliton width at a particular wavelength λ in a given material (of n_b, r_{eff}, and κ_{eff}) and the ratio between the soliton peak intensity and the background irradiance (the so-called intensity ratio). The existence curve is a common property of all solitons: It gives the relationship among the soliton's amplitude, width, nonlinearity, and optical wavelength in the medium. For Kerr solitons the existence curve is simple and is a monotonically decreasing function of peak intensity for both bright and dark solitons. For screening solitons[13,15] the existence curves of dark and bright solitons are very different from each other for peak (normalized) intensities larger than unity (because of different boundary conditions). As is shown below, the existence curves for photovoltaic dark and bright solitons resemble each other only in the $J = 0$ case.

In the limit of low intensity ratio, $u_\infty^2 \ll 1$, one can get an approximate analytic solution for the soliton waveforms for both open- and closed-circuit cases. In this limit and for $\Delta x/l \ll 1$, the maximum current is $J = u_\infty^2$. Equation (25) becomes

$$u'' = -(u_\infty^2 - u^2)u, \tag{27}$$

with boundary conditions $u(0) = 0$ and $u'(0) = p_0 = u_\infty^2/\sqrt{2}$. The normalized propagation constant $\delta \to 0$, which implies that, in this limit, all dark solitons propagate at the same velocity with a propagation constant equal to that of a plane wave propagating in the same crystal at the absence of the photovoltaic effect. The solutions of Eq. (27) are the usual solutions for Kerr-type dark solitons: $u(\xi) = u_\infty \tanh(u_\infty \xi/\sqrt{2})$.

Finally, we point out that to date only dark photovoltaic solitons have been observed in the open-circuit realization.[35,36] The experiments were carried out with a finite notch-bearing beam (which covers only a rather small region in the crystal), and the natural dark irradiance (I_{dark}) was used without background illumination. The soliton peak intensity was much larger than the dark irradiance; thus the experiments were done in the intensity regime where an increase in the intensity (with all other parameters unchanged) should have made the dark soliton wider, as expected from the upper curve in Fig. 6. This did not happen, and instead the dark soliton became gray (i.e., with a nonzero intensity at the center of the dark notch). The reason for the discrepancy between the experiments and the theory is that a dark soliton borne on a finite beam (as was used in that experiment) gives rise to circulation currents (around the beam) that are inherently two dimensional; thus the scalar analysis (the assumption that **J** and **E** are parallel to x) is no longer valid. Similar observations were found with dark screening solitons: the existence curve of dark solitons was verified experimentally[20] with dark solitons borne on infinite beams (which cover the entire crystal), and it agrees very well with that in the theory,[15] whereas dark solitons borne on finite beams in biased photorefractive crystals could be observed in quasi-steady state[10] but not in steady state.[20] Experiments with notch-bearing infinite beams targeted to yield the existence curve of dark photovoltaic solitons are currently under way.

6. BRIGHT SOLITONS

For bright solitons one requires three boundary conditions: (i) $u_\infty = u'(\infty) = u''(\infty) = 0$, (ii) $p_0 = 0$, and (iii) $u''(0)/u_0 < 0$. The first ensures the decay of the wave function and all its derivatives far from $\xi = 0$, and the second and the third ensure a local maximum at $\xi = 0$. Taking the limit $\xi \to \infty$ in Eq. (23) leads to $\delta = 1 - (J + 1)\ln(u_0^2 + 1)/u_0^2$. This means that δ now depends on u_0^2 and J. Recalling the possible values of J for bright solitons (Section 4), which implies that $0 \leqslant J \leqslant (\Delta x u_0^2)/[l(1 + u_0^2)] \leqslant \Delta x/l \approx 0.001$, we notice that $\delta > 0$ for all $u_0 > 0.05$, whereas for smaller values of u_0, δ becomes negative.

Substituting for δ, setting $\xi = 0$ in Eq. (22), and imposing boundary condition (iii) show that only the upper (positive) sign can give rise to bright solitons, implying that bright photovoltaic solitons can be generated with a positive Δn_0 only. Notice that, although δ reverses sign near $u_0 \approx 0.05$, the required Δn_0 is positive for all values of u_0.

Therefore, bright photovoltaic solitons are solutions of

$$u'' = \left(\delta + \frac{J - u^2}{1 + u^2}\right)u, \tag{28}$$

with $u(0) = u_0$, $u'(0) = 0$, and $\delta = 1 - (J + 1)\ln(u_0^2 + 1)/u_0^2$ or, alternatively [if we substitute for δ and choose the upper sign in Eq. (23)], of

$$u' = \left\{(J + 1)\left[\ln(u^2 + 1) - \frac{u^2}{u_0^2}\ln(u_0^2 + 1)\right]\right\}^{1/2}, \tag{29}$$

with $u(0) = u_0$. We notice that in both Eqs. (28) and (29) and in the expression for δ the term $J + 1$ appears. However, for bright solitons J lies between 0 and 0.001. We therefore expect that they will have only a minor effect on the solitons as long as u_0 is larger than 0.05, the point at which the propagation constant reverses sign. We integrate Eq. (28) numerically for various values of u_0 and for $J = 0$ and $J = J_{\max} = 0.001/(1 + u_0^2)$ and obtain the waveforms $u(\xi)$ of bright photovoltaic solitons. We indeed find no significant difference between the open- and closed- circuit cases; both are identical to the

waveforms shown in Ref. 34. Equation (28) can also be integrated numerically to show the soliton existence curve: the full width at half-maximum of u^2 as a function of the ratio between its peak amplitude and the square root of the background irradiance (u_0). We show this function in Fig. 7 for u_0 from 0.5 to 10. The curves for $J = 0$ and $J = J_{max} = 0.001/(1 + {u_0}^2)$ coincide with each other (within the resolution of the plot), implying that the bright photovoltaic soliton is not affected by the external resistor (or by the value of the current in the circuit) as long as its intensity ratio u_0 is larger than 0.05.[51]

It is now important to discuss the $u_0 < 0.05$ regime, which seems to be slightly different because δ is negative there. Before we even specify the value of J for bright solitons, Eq. (22) in this regime (of $u^2 \ll 1$) becomes

$$u'' = \pm[(\delta + J) - (J + 1)u^2]u. \tag{30}$$

Integrating Eq. (30) by quadrature and substituting conditions (i) and (ii) implies that $\delta = {u_0}^2/2 - J$. However, imposing condition (iii) and using Eq. (30) and δ reveal that the proper sign for bright solitons is still the upper sign, unaffected by the sign change in δ near $u_0 \approx 0.05$. Using the maximum allowed value for $J_{max} \cong 0.001/(1 + {u_0}^2)$, we can simplify Eq. (30) into

$$u'' = ({u_0}^2/2 - u^2)u, \tag{31}$$

with $u(0) = u_0$ and $u'(0) = 0$. The solutions of Eq. (31) are $u(\xi) = u_0 \operatorname{sech}(u_0\xi/\sqrt{2})$, which are identical to Kerr-type solitons. Interestingly enough, in this limit of $u^2 \ll 1$ the approximate equation in the $J = 0$ case is identical to that of $J = J_{max}$ [Eq. (31)] and of course provides the same (analytic, Kerr-like) solutions for the soliton waveforms. This means that the waveforms of the bright photovoltaic solitons are unaffected by the presence of current (or of a passive external resistor). There is, however, an important difference between the induced waveguides [induced refractive-index change, $\Delta n(\xi)$]. For $J = 0$, $\Delta n(\xi) \propto -E(\xi)$ is positive to all ξ, whereas for $J = J_{max}$, $\Delta n(\xi)$ crosses zero at some point and becomes negative for $|\xi|$ larger than some (nonzero) value. At this point it is instructive to look at the difference between the refractive-index changes for the two cases:

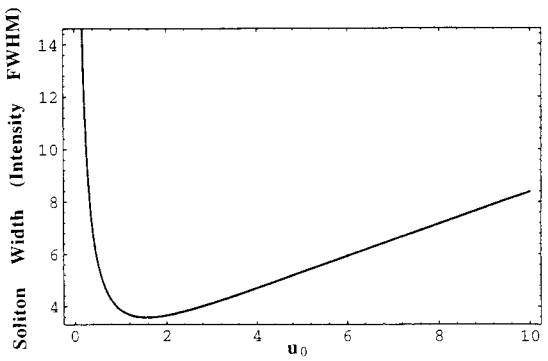

Fig. 7. Soliton existence curve for open-circuit and closed-circuit bright photovoltaic solitons (the curves coincide everywhere). The curves show the soliton width (FWHM of the intensity, u^2) in units of $\Delta x {k_0}{n_b}^2(r_{eff}E_p r)^{1/2}$ as a function of peak soliton amplitude u_0, k_0 being the wave number in vacuum.

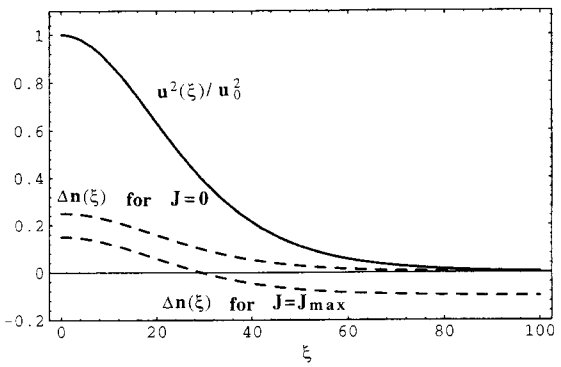

Fig. 8. Soliton intensity waveforms $u^2(\xi)$ (solid curve) and the induced change in the refractive index [$100 \times \Delta n(\xi) \propto -E(\xi)$] for $u_0 = 0.05$ and $J = 0$ and $J = J_{max}$. The waveforms $u^2(\xi)$ coincide with each other everywhere, whereas the $\Delta n(\xi)$ curves are offset by a constant parameter equal to J_{max}.

$$\Delta n(\xi)_{|J=0} - \Delta n(\xi)_{|J=J_{max}}$$

$$\propto [-E(\xi)_{|J=0}] - [-E(\xi)_{|J=J_{max}}]$$

$$= \frac{u^2}{1 + u^2} - \left(-\frac{J - u^2}{1 + u^2}\right) = \frac{J}{1 + u^2},$$

which, for $u^2 \ll 1$, is simply equal to the (constant) current, J. This means that the soliton-induced waveguides are identical in their shape and dimensions, yet they are shifted (offset) with respect to each other, the offset being equal to the current J. This explains why the waveforms of the solitons, which are identical to the waveforms of the fundamental guided mode in each of the waveguides,[52] are identical in both cases. For example, consider the cases of $J = 0$ and $J = J_{max} = 0.001/(1 + {u_0}^2)$ for a peak amplitude of $u_0 = 0.05$. The soliton intensity waveforms [$u^2(\xi)$; solid curve] and $100 \times \Delta n(\xi)$ (dashed curves) for both cases [as obtained by solution of Eq. (28)] are shown in Fig. 8. The waveforms coincide with each other, whereas the $\Delta n(\xi)$ curves are offset by a constant parameter (equal to J_{max}), the upper (lower) curve corresponding to the $J = 0$ ($J = J_{max}$) case.

Having examined the entire range of u_0, we conclude that bright photovoltaic solitons of either open or closed circuit obey the existence curve of Fig. 7. This means that the waveforms of the solitons of the two cases coincide with each other. Obviously, this observation implies that, in contrast to the dark photovoltaic solitons, bright photovoltaic solitons are not favorable for switching applications.[53]

Finally, we note that bright photovoltaic solitons have not been observed yet. The reason for this is simple: The first attempts to observe photovoltaic solitons were done in $LiNbO_3$, which possesses the largest known photovoltaic nonlinearity. However, in all $LiNbO_3$ crystals the refractive-index change caused by the photovoltaic effect is always negative ($\Delta n_0 < 0$), which can give rise to dark solitons only.[35,36] We expect that bright photovoltaic solitons will be observed in crystals other than $LiNbO_3$ in the near future.

7. CONCLUSIONS

We have analyzed dark and bright solitons in open- and closed-circuit photorefractive–photovoltaic media. We have shown that the new effects added by permitting a nonzero current modify the parameters of the solitons, having a rather dramatic effect on dark solitons and a small effect on bright solitons. This effect can be used for switching[54]: in the ON situation the operation point lies on the existence curve, whereas in the OFF case it moves away from the curve. In general, this switching method should be useful mostly at large intensity ratios (u_∞ larger than 5) where even small changes in the current completely modify the existence curve. At intensity ratios smaller than unity we do not expect efficient switching because all solitons can tolerate changes within a few percent in their parameters. An experimental study of these predictions is currently under way.

ACKNOWLEDGMENT

We are in debt to Charalambo Anastassion of Princeton University for finding and correcting arithmetic errors in our paper. M. Segev gratefully acknowledges the support of the National Science Foundation and of the U.S. Army Research Office.

*Present address, Advanced Functional Materials Research Center, Shin-Etsu Chemical Corporate, Gunma, Japan.

REFERENCES AND NOTES

1. In this paper, as in all our other papers on self-trapping of optical beams in photorefractive media, we use the term "soliton" in conjunction with nondiffracting self-trapped optical beams. That is, we use the broader definition of solitons that includes those in nonintegrable systems, as defined by V. E. Zakharov and B. A. Malomed, in *Physical Encyclopedia*, A. M. Prokhorov, ed. (Great Russian Encyclopedia, Moscow, 1994), p. 571, and also as discussed in detail by V. G. Makhankov in his review paper, Phys. Rep. **35**, 1 (1978).
2. M. Segev, B. Crosignani, A. Yariv, and B. Fischer, Phys. Rev. Lett. **68**, 923 (1992).
3. B. Crosignani, M. Segev, D. Engin, P. DiPorto, A. Yariv, and G. Salamo, J. Opt. Soc. Am. B **10**, 449 (1993).
4. G. Duree, J. L. Shultz, G. Salamo, M. Segev, A. Yariv, B. Crosignani, P. DiPorto, E. Sharp, and R. Neurgaonkar, Phys. Rev. Lett. **71**, 533 (1993).
5. M. Segev, A. Yariv, G. Salamo, G. Duree, J. Shultz, B. Crosignani, P. DiPorto, and E. Sharp, Opt. Photon. News **4**(12), 8 (1993).
6. M. Segev, A. Yariv, B. Crosignani, P. DiPorto, G. Duree, G. Salamo, and E. Sharp, Opt. Lett. **19**, 1296 (1994).
7. G. Duree, G. Salamo, M. Segev, A. Yariv, B. Crosignani, P. DiPorto, and E. Sharp, Opt. Lett. **19**, 1195 (1994).
8. D. N. Christodoulides and M. I. Carvalho, Opt. Lett. **19**, 1714 (1994).
9. M. Segev, G. Salamo, G. Duree, M. Morin, B. Crosignani, P. DiPorto, and A. Yariv, Opt. Photon. News **5**(12), 9 (1994).
10. G. Duree, M. Morin, G. Salamo, M. Segev, A. Yariv, B. Crosignani, and P. DiPorto, Phys. Rev. Lett. **74**, 1978 (1995).
11. M. Morin, G. Duree, G. Salamo, and M. Segev, Opt. Lett. **20**, 2066 (1995).
12. M. Segev, G. C. Valley, B. Crosignani, P. DiPorto, and A. Yariv, Phys. Rev. Lett. **73**, 3211 (1994).
13. D. N. Christodoulides and M. I. Carvalho, J. Opt. Soc. Am. B **12**, 1628 (1995).
14. S. R. Singh and D. N. Christodoulides, Opt. Commun. **118**, 569 (1995).
15. M. Segev, M. Shih, and G. C. Valley, J. Opt. Soc. Am. B **13**, 706 (1996).
16. Steady-state self-focusing effects in biased photorefractive crystals were first observed by M. D. Iturbe-Castillo, P. A. Marquez-Aguilar, J. J. Sanchez-Mondragón, S. Stepanov, and V. Vysloukh, Appl. Phys. Lett. **64**, 408 (1994).
17. Screening solitons were first observed by M. Shih, M. Segev, G. C. Valley, G. Salamo, B. Crosignani, and P. DiPorto, Electron. Lett. **31**, 826 (1995).
18. M. Shih, P. Leach, M. Segev, M. Garrett, G. Salamo, and G. C. Valley, Opt. Lett. **21**, 324 (1996).
19. K. Kos, H. Ming, G. Salamo, M. Shih, M. Segev, and G. C. Valley, Rapid Comm., Phys. Rev. E **53**, R4330 (1996).
20. Z. Chen, M. Mitchell, M. Shih, M. Segev, M. Garrett, and G. C. Valley, Opt. Lett. **21**, 629 (1996).
21. Z. Chen, M. Mitchell, and M. Segev, Opt. Lett. **21**, 716 (1996).
22. M. D. Iturbe-Castillo, J. J. Sanchez-Mondragón, S. I. Stepanov, M. B. Klein, and B. A. Wechsler, Opt. Commun. **118**, 515 (1995).
23. M. Shih, M. Segev, and G. Salamo, Opt. Lett. **21**, 931 (1996).
24. M. Shih and M. Segev, Opt. Lett. **21**, 1538 (1996).
25. M. Shih, Z. Chen, M. Segev, T. Coskun, and D. N. Christodoulides, Appl. Phys. Lett. **69**, 4151 (1996).
26. H. Meng, G. Salamo, M. Shih, and M. Segev, Opt. Lett. **22**, 448 (1997); W. Krolikowski and S. A. Holstrom, Opt. Lett. **22**, 369 (1997); and G. C. Garcia-Quirino, M. D. Iturbe-Castillo, V. A. Vysloukh, J. J. Sanchez-Mondragon, S. I. Stepanov, G. Lugo-Martinez, and G. E. Torres-Cisneros, Opt. Lett. **22**, 154 (1997).
27. M. Segev, G. C. Valley, S. R. Singh, M. I. Carvalho, and D. N. Christodoulides, Opt. Lett. **20**, 1764 (1995).
28. S. R. Singh, M. I. Carvalho, and D. N. Christodoulides, Opt. Lett. **20**, 2177 (1995).
29. M. I. Carvalho, S. R. Singh, and D. N. Christodoulides, Phys. Rev. E **53**, R53 (1996).
30. D. N. Christodoulides, S. R. Singh, M. I. Carvalho, and M. Segev, Appl. Phys. Lett. **68**, 1763 (1996).
31. W. Krolikowski, N. Akhmediev, and B. Luther-Davies, Opt. Lett. **21**, 782 (1996).
32. Z. Chen, M. Segev, T. Coskun, and D. N. Christodoulides, Opt. Lett. **21**, 1436 (1996).
33. Z. Chen, M. Segev, T. Coskun, D. N. Christodoulides, Y. Kivshar, and V. V. Afanasjev, Opt. Lett. **21**, 1821 (1996).
34. G. C. Valley, M. Segev, B. Crosignani, A. Yariv, M. M. Fejer, and M. Bashaw, Phys. Rev. A **50**, R4457 (1994).
35. M. Taya, M. Bashaw, M. M. Fejer, M. Segev, and G. C. Valley, Phys. Rev. A **52**, 3095 (1995).
36. M. Taya, M. C. Bashaw, M. M. Fejer, M. Segev, and G. C. Valley, Opt. Lett. **21**, 943 (1996).
37. M. Chauvet, S. A. Hawkins, G. Salamo, M. Segev, D. F. Bliss, and G. Bryant, Opt. Lett. **21**, 1333 (1996).
38. M. Mitchell, Z. Chen, M. Shih, and M. Segev, Phys. Rev. Lett. **77**, 490 (1996).
39. D. N. Christodoulides, T. H. Coskun, M. Mitchell, and M. Segev, Phys. Rev. Lett. **78**, 646 (1997).
40. S. Gatz and J. Herrmann, J. Opt. Soc. Am. B **8**, 2296 (1991).
41. G. C. Valley and J. Lam, in *Photorefractive Materials and Their Applications I*, P. Gunter and J. P. Huignard, eds. (Springer-Verlag, New York, 1988), Chap. 3.
42. H. J. Eichler, P. Gunter, and D. W. Pohl, *Laser-Induced Dynamic Gratings* (Springer-Verlag, New York, 1986).
43. B. I. Sturman, E. Shamonina, M. Mann, and K. H. Ringhofer, J. Opt. Soc. Am. B **12**, 1642 (1995).
44. B. I. Sturman and V. M. Fridkin, in *The Photovoltaic and Photorefractive Effect in Non-Centrosymmetric Materials* (Gordon & Breach, Philadelphia, Pa., 1992).
45. We note that photovoltaic gray solitons, which propagate at some angle with respect to the optical axis z, are also possible. In fact, the Y-junction solitons observed in the research reported Ref. 36 can be considered a gray pair once the channels are well separated. The theory of photovol-

taic gray solitons resembles that of gray screening solitons (described in Ref. 13).
46. More-complicated configurations can lead to tensor effects and to vector solitons, as described in Ref. 25.
47. As explained in Ref. 44, photovoltaic current must be driven by a real optical field (photons) and cannot be driven by thermal excitations. The main argument is that the photovoltaic current is fundamentally a polar current, rather than noise in the current as I_{dark} is. If photovoltaic dark irradiance could exist, it would permit polar currents driven by temperature and thereby perpetual-motion machines.
48. S. Orlov, A. Yariv, and M. Segev, Appl. Phys. Lett. **68**, 1610 (1996).
49. In fact, the most significant correction factor is to Eq. (8), which leads to self-bending effects. For screening solitons, self-bending was predicted in Ref. 14 and observed in the research reported Refs. 18, 24, 25, and 32).
50. S. Gatz and J. Herrmann, IEEE J. Quantum. Electron. **28**, 1732 (1992).
51. We note that a small negative offset in the induced refractive index profile $\Delta n(\xi)$ caused by nonzero current is present in the closed-circuit case. This means that far away from $\xi = 0$, Δn becomes negative. However, at $u_0 > 0.05$ this effect is almost unnoticeable.
52. The idea to treat solitons as the guided modes of the waveguides that they induce was pioneered by A. W. Synder and A. P. Sheppard, Opt. Lett. **18**, 482 (1993) and by Y. Silberberg, "Self-induced waveguide: spatial optical solitons," in *Anisotropic and Nonlinear Optical Waveguides*, G. C. Someda and G. I. Stegeman, eds. (Elsevier, Amsterdam, 1992). See also the review by A. W. Synder, D. J. Mitchell, and Y. Kivshar, Mod. Phys. Lett. B **9**, 1479 (1995).
53. This observation is true in steady state only. We expect that, if a bright photovoltaic soliton at $u_0 \leq 0.1$ is switched from $J = 0$ to $J = J_{max}$, there will be a transient effect, because the induced refractive index $\Delta n(\xi)$ has to readjust to a new offset value, as shown in Fig. 8.
54. Switching of solitons by use of a change in a single parameter that causes large deviations in the existence curve was used in the coupled soliton pairs experiments of Refs. 32 and 33.